JACS
JOURNAL OF THE AMERICAN CHEMICAL SOCIETY

Communication

pubs.acs.org/JACS

Ab Initio Study of the Emissive Charge-Transfer States of Solvated Chromophore-Functionalized Silsesquioxanes

Shaohui Zheng, Heidi Phillips, Eitan Geva,* and Barry D. Dunietz*

Department of Chemistry, University of Michigan, Ann Arbor, Michigan 48109, United States

Supporting Information

ABSTRACT: Recent experimental advances in the ability to tune the optical properties of silsesquioxanes by functionalizing them with photoactive ligands have made these compounds attractive candidates for building blocks of photovoltaic materials. We employ state-of-the-art *ab initio* methodologies to determine the nature of the excited charge-transfer (CT) states that give rise to a large red-shift between absorption and emission in these molecules, in comparison to the corresponding red-shift in the individual ligand. The calculations are based on time-dependent density functional theory and employ the recently developed Baer−Neuhauser−Livshits range-separated hybrid (RSH) functional. Solvent effects are accounted for via a combination of charge-constrained density functional theory and the polarizable continuum model. We find that the experimentally observed red-shift is consistent with identifying the emissive state as a *ligand-to-ligand*, rather than a *ligand-to-silsesquioxane*, CT state. We also find that the enhanced red-shift cannot be explained without accounting for solvation effects, and we demonstrate the importance of using a RSH functional to obtain reliable predictions regarding the emissive state.

The ability to tune the electronic and photonic properties of silsesquioxanes (SQ) by functionalizing them with different ligands has recently made them attractive candidates for photovoltaic and optical applications.[1] These compounds have also been studied computationally at various levels of theory.[2] One of the most striking spectroscopic observations pertaining to these compounds is the significant increase in the red-shift of the emission spectrum, relative to the absorption spectrum, that occurs upon ligation.[1b,c] For example, whereas the red shift in stilbene is ∼0.3 eV, that of stilbene-functionalized octahedral silsesquioxane (OHSQ) is ∼0.8−0.9 eV.[1c] The emission spectrum of the SQ-coupled chromophores is strongly red-shifted, while the absorption spectrum remains similar to that of the isolated stilbene. This suggests that while the absorption spectrum is dominated by excitations which are localized on the ligand, the increase in the red-shift is associated with the emergence of low-lying emissive states that extend beyond a single ligand. The fact that the red-shift increases with increasing polarizability of the solvent[3], also suggests that these emissive states involve extensive charge-transfer (CT) character.

Our goal in this paper is to elucidate the nature of the emissive CT states in functionalized SQs using state-of-the-art density functional theory (DFT) techniques. To this end, we employed time-dependent DFT (TD-DFT) and the Tamm−Dancoff approximation (TDA)[4], with the recently developed range-separated hybrid (RSH) functional of Baer−Neuhauser−Livshits (BNL).[5] We present a state-of-the-art approach to address the solvation effects on the CT states. We combine charge-constrained DFT (C-DFT)[6] optimizations with novel polarizable continuum models (PCM)[7], implementing the switching/Gaussian (SWIG) method.[8] We successfully benchmark our scheme against the experimental emission spectrum.

All the calculations reported here were carried out within version 4.0 of the Q-Chem program package[9] and using the 6-31G* basis set. We use the B3LYP functional[10] for all the geometry optimizations described below. In calculating the BNL γ parameter, we use the $J(\gamma)$[11] scheme. [Additional information on the BNL parametrization scheme is provided in the references and in the Supporting Information (SI), where we also provide the γ values and $J(\gamma)$ plots for the models studied below (Figure SI-1).] The PCM dielectric constant was set equal to that of tetrahydrofuran (THF), $7.43\varepsilon_0$ which is the solvent used in the experiment.[1c]

The ground-state trends reflected in the molecular orbital energies are essential for understanding the electronic spectra and the roles of the SQ and chromophore as electron acceptor and donor, respectively. In particular, the highest occupied and lowest unoccupied molecular orbital (HOMO−LUMO) gaps must correspond to the fundamental gap[12] (the difference between the ionization potential and the electron affinity), which is taken into account by obtaining the correct BNL γ parameter. Indeed, we recently showed that TD-DFT with the BNL functional reproduces well the experimental absorption spectra for a wide range of functionalized OHSQs.[13] We also found that for the system under study here, the absorptive excitations are localized on the stilbene ligands. In the present paper, we address the significantly more challenging problem of identifying the emissive CT state and quantitatively predicting its energy relative to the absorptive state.

We demonstrate that the combined RSH-CDFT-PCM scheme as implemented in this report yields predictions related to CT processes which are in excellent agreement with experiment. This is contrasted with the results obtained using more traditional functionals, such as B3LYP, which are known to significantly underestimate the energy of CT states. In general, we have found that TDA provides a slightly better agreement with experiment in reproducing the absorption

Received: February 18, 2012
Published: April 16, 2012

spectra with ~0.2 eV higher excitation energies than TD-DFT. For completeness, both the TDA and TD-DFT excitation energies are listed in Table SI-1. This comparison between TDA and the TD-DFT is indicated in previous studies.[14] We continue below with TDA and note that the CT excited-state energies are found to have even smaller differences between the TDA and the TD-DFT energies.[4,14,15]

The current study is focused on OHSQ functionalized with *trans*-stilbene that has been shown to result in a large shift of the emission spectrum of up to 0.9 eV.[1c] The systems studied via experimental methods are assumed to be fully functionalized by eight chromophores, as shown on the left side in Figure 1.[1b,c] Two CT pathways may explain the red-shift in the

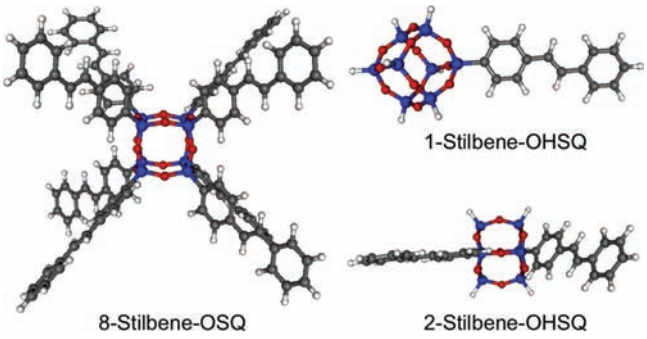

Figure 1. SQ fully functionalized with eight stilbene ligands (left). Molecular models of 1-stilbene-OHSQ and 2-stilbene-OHSQ (right).

emission spectrum. The first involves CT from the chromophore to the SQ core, and the second is solvent-mediated CT between chromophores. However, it remains unclear which of these pathways is relevant to the red-shifted emission. We emphasize that the CT between chromophores can be intramolecular, involving chromophores attached on the same SQ molecule, or intermolecular, within aggregates of the functionalized SQs.

To answer this open question concerning CT, we use one and two *trans*-stilbene-functionalized OHSQ as models, referred to as 1-stilbene-OHSQ and 2-stilbene-OHSQ, respectively (right side in Figure 1). In the 2-stilbene-OHSQ, the chromophores are added at two nearest-neighbor Si sites, where the strongest coupling is expected. The energies of the HOMOs and LUMOs of the OHSQ, stilbene, 1-stilbene-OHSQ, and 2-stilbene-OHSQ are listed in Table 1.

Table 1. BNL HOMO and LUMO Energies (eV)[a]

	$HOMO_s$	$LUMO_s$	$HOMO_o$	$LUMO_o$
trans-stilbene	−6.67	0.71	–	–
OHSQ	–	–	−9.42	2.10
1-stilbene-OHSQ	−6.86	0.35	−9.14	2.07
2-stilbene-OHSQ	−6.78	0.33	−8.95	2.10

[a]Subscript "s" refers to stilbene and subscript "o" to the OHSQ cage.

Importantly, we find that the chromophore gap is substantially lower than the OHSQ, with a 1.4 eV lower LUMO energy. We note that the chromophore-localized LUMO in the functionalized SQ system is stabilized by 0.3 eV; however, the LUMO localized on the SQ remains at a higher energy.

We begin by considering the *gas-phase* vertical electronic excitation energies for stilbene-OHSQ at the solvated ground-state geometry (i.e., the optimized ground-state structure obtained within PCM at the B3LYP level). The excitation energies obtained via TDA using the BNL and B3LYP functionals are shown in Figure 2. A list of the TDA excited states energies is provided in Table SI-1.

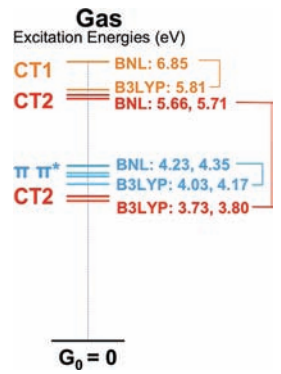

Figure 2. Gas-phase vertical TDA electronic excitation energies for 2-stilbene-OHSQ at the solvated ground-state geometry.

The excitations can be classified into three different types: (1) $\pi-\pi^*$ excitations localized on the stilbene ligands; (2) CT1 excitations that involve CT between stilbene and OHSQ; and (3) CT2 excitations that involve CT from one stilbene to another stilbene. We report the CT1 energies calculated with the 1-stilbene-OHSQ model and CT2 energies calculated with the 2-stilbene-OHSQ model (see Figure 1). We find that the two CT1 energies calculated using the 2-stilbene-OHSQ model are in good agreement with the CT1 energy of the 1-stilbene-OHSQ model. In our current study, the 2-stilbene-OHSQ model represents CT2 excitations between chromophores on the same SQ molecule and CT between chromophores within aggregates of functionalized SQs. The energetics of the CT states is expected to remain qualitatively the same with models that explicitly address the possibility of aggregates.

The $\pi-\pi^*$ excitations with the larger oscillator strengths dominate the absorption spectra and have been studied extensively recently.[13] The BNL energies of these absorbing states are 0.2 eV higher than the B3LYP values.[13] The CT states are characterized by oscillator strengths which are significantly smaller than those of the $\pi-\pi^*$. The CT excited states are classified as either CT1 or CT2, based on the corresponding attachment and detachment densities,[16] as shown in Figure 3. The $\pi-\pi^*$ excitations are identified with HOMO-to-LUMO replacements occurring on the same chromophore unit. The CT2 state involves mainly HOMO-to-LUMO replacements where the orbitals are related to

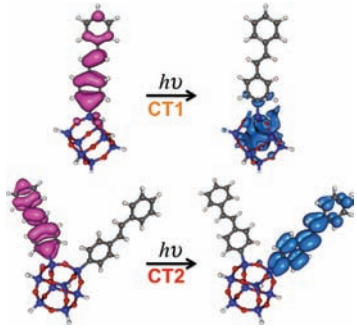

Figure 3. CT1 and CT2 detachment and attachment densities.

dx.doi.org/10.1021/ja301442v | J. Am. Chem. Soc. 2012, 134, 6944−6947

different chromophores. Finally, the CT1 state is dominated by replacement of the chromophore HOMO by the SQ-LUMO.

Both CT1 and CT2 excited-state energies obtained via BNL are significantly higher than those obtained via B3LYP. This is consistent with the well-documented tendency of B3LYP to overstabilize CT states.[12,17] The gas-phase CT1 energies obtained with both BNL and B3LYP functionals are observed to be significantly higher than the corresponding $\pi-\pi^*$ excited-state energy. This implies that the CT1 state does not affect the emission spectrum following the $\pi-\pi^*$ excitations. The situation is quite different for the CT2 state, however.

The B3LYP functional indicates that the CT2 state affects the emission spectrum, where the CT2 energy lies below the corresponding $\pi-\pi^*$ energy. However B3LYP is known to underestimate the energies of CT states, and therefore the low CT2 energy observation cannot be used to conclusively indicate the CT2 state as the low-lying emissive state. Indeed, the CT2 states at the gas phase are indicated to lie significantly above the $\pi-\pi^*$ by BNL. We proceed with BNL, which is expected to be more reliable for CT states. In the next step, we consider solvation that strongly affects the CT state energies.

The relatively strong dependence of the emission spectrum on solvent polarity[1b] indicates that the emissive state energies are strongly influenced by solvation. We consider the solvation effect on the excited states by starting with the vertical excitations at the solvated ground-state geometry, then allowing for solvated charge-separated state geometry relaxation using C-DFT. We evaluate the CT state solvation energies from the difference between the C-DFT/PCM energy and the gas-phase C-DFT energy *at the same solvated molecular geometry* (particular to each CT type): $E_{solv}^{CT} = E(\text{C-DFT/PCM}) - E(\text{C-DFT/gas})$. The C-DFT relaxations use charge constraints ranging from the subunit partial charges at the gas-phase TDA level to the limit where a whole electron is transferred. The TDA charges correspond to the Mulliken atomic populations of the CT state. We find that the donor chromophore in the CT1 and CT2 at the ground-state geometry is charged 0.84 and 0.95, respectively, where 1.0 indicates the complete electron-transfer limit. For CT1 we consider the fragment charges of the chromophore (donor) and the SQ unit (acceptor), and for CT2 we define the constraints to apply on the sum of the atomic charges of the two chromophores, designating one as the donor and the other as the acceptor.

The solvated excited-state energies are shown in Figure 4. A list of the corresponding energies is provided in Table SI-2. We first consider the solvated excited-state energies at the solvated ground-state geometry. As expected, solvation gives rise to significant stabilization of both CT1 and CT2 states. However, even with this extra stabilization, the CT1 energy remains significantly higher than that of the non-CT $\pi-\pi^*$ state. At the same time, the solvation lowers the CT2 state energy below that of the $\pi-\pi^*$ state by up to 0.1 eV at the solvated ground-state geometry, which suggests that CT2 is the emissive state, rather than CT1.

We focus next on the relaxation processes following the electronic excitation that result in an even larger red-shift between absorption and emission. The different types of energy contributions to the relaxation are illustrated in the inset in Figure 4. The intramolecular reorganization energies affecting the emission spectrum include the stabilization of the excited state (λ_e) and destabilization at the ground electronic level (λ_g). An additional third term, ΔE_0, is the energy difference between the absorbing and emitting excited states. Here the energy

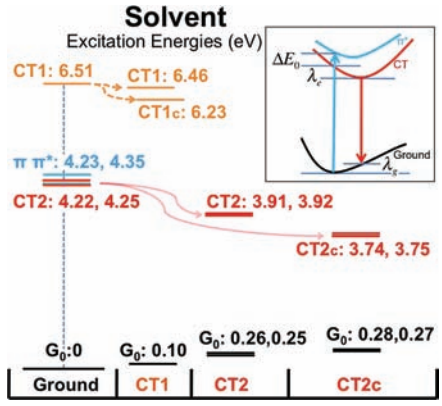

Figure 4. Solvated electronic excitation energies (eV), accounting for intramolecular reorganization. G_0 is the ground state energy. Molecular geometries: ground- solvated ground-state geometry; CT(1,2)- solvated CT(1,2) with TDA partial-charge constraints; CT(1,2)c- solvated CT(1,2) with complete electron-transfer constraints.

difference is between the vertical excited states at the solvated and unrelaxed ground-state geometry. The overall red-shift of the emission spectra, therefore, becomes $\Delta E = \lambda_g + \lambda_e + \Delta E_0$.

The solvated electronic-state energies at the CT state optimized structures are also illustrated in Figure 4 and Table SI-2. For the CT2 case, we consider the two possible transfer directions (CT to and from each chromophore), where the symmetry breaking effect due to SQ binding results in slightly different energies for the two directions. We therefore performed geometry optimization for each CT2 state separately.

We consider the intramolecular reorganization energies for the CT states, where the geometry optimization was carried out only with respect to the ligands while keeping the OHSQ in its ground-state geometry. Full optimization leads to a distortion of the SQ unit, which we believe to be a nonphysical artifact of using a continuum model for solvation. More specifically, the attraction between the positively and negatively charged ligands tends to bring them together more than they would be in a molecular liquid, where the solvent molecules would keep them farther apart. As a result, the SQ unit is distorted more than it would have been in a molecular liquid. In addition, it is important to note that even when full optimization is carried out, the CT1 state energy remains substantially higher than the absorbing state energy. On the other hand, we find that the intramolecular reorganization associated with the CT2 states lowers their energies by more than 0.3 eV.

Another contribution to the emission spectral shift is the corresponding destabilization of the ground electronic state, which is close to 0.3 eV for either of the CT2 optimized geometries. Interestingly, the relaxation terms are effectively the same for the two CT2 states. The contribution to the spectral red-shift due to excited-state energy differences (ΔE_0) is 0.1 eV for the first state and almost vanishing for the second state. Therefore, the 0.1 eV energy split emerges from the difference between the two low-lying $\pi-\pi^*$ excitations, where the SQ binding induces symmetry breaking in the absorption energies.

The solvation, where the partial charges from the BNL TDA gas-phase calculation are used to define the constraints in the C-DFT, indicates significant CT stabilization. However, as summarized in Table 2, the predicted shift still does not account for the experimentally observed red-shift in the emission spectrum. Indeed, the solvation may stabilize the

dx.doi.org/10.1021/ja301442v | J. Am. Chem. Soc. 2012, 134, 6944−6947

Table 2. Modeled Relaxation Energies (eV) of the Electronic Charge-Transfer States and Their Difference from the Excitonic $\pi-\pi^*$ Energy at the Ground-State Geometry[a]

	relaxation energy			
electronic state	λ_e	λ_g	ΔE_0	ΔE
$\pi-\pi^*$	0.10	0.17	0.00	0.27
	0.06	0.12	0.00	0.18
CT1(0.84)	0.05	0.10	−2.16	–
CT2(0.95)	0.31	0.26	0.13	0.70
	0.33	0.25	−0.02	0.56
CT2(1)	0.48	0.28	0.13	0.89
	0.50	0.27	−0.02	0.75

[a]A negative sign on ΔE_0 means a higher energy. The sum of the relaxation energy and the ΔE_0 defines the overall emission spectra shift, ΔE. For the electronic states, in parentheses we specify the charge on the donor designated chromophore used in the corresponding C-DFT calculations.

transfer of a whole electron; therefore, we consider the electronic CT2 state upon a complete electron transfer. We assign the charge constraints 1.0 and −1.0 for the donor and acceptor, respectively. We denote this state as CT2c and illustrate the corresponding energy levels on the right side of Figure 4. (A list of the corresponding energies is provided in Table SI-3.) The solvation energies corresponding to the complete electron transfer increase for either of the CT states by 0.2 eV. The destabilization of the ground state at the new geometry, however, remains almost unchanged. We therefore find that the stabilization of the CT2c state is twice the destabilization of the ground-state energy.

The resulting red-shift between absorption and emission spectra for the CT2 state represented by the CT2c model adds up to 0.8 and 0.9 eV, which is in excellent agreement with the experimental values of 0.8 and 0.9 eV.[1c] This suggests that the polarizable nature of the solvent increases the partial charges in solution beyond their values as obtained from the gas-phase calculation, thereby leading to further stabilization of the CT states. We list the different energy contributions to the spectral shift in Table 2. We include for comparison the relaxation energies of the CT1 state but emphasize again that only CT2 is indicated to be lowered enough by the solvent to potentially play the role of the emissive state in the relaxation process of the $\pi-\pi^*$ state.

To summarize, in this Communication, we *quantitatively* reproduce the enhanced red-shift between the absorption and emission spectra of stilbene-functionalized OHSQs using a strategy that combines TD-DFT/TDA with the BNL RSH functional and accounts for solvation effects via C-DFT and PCM. We identify the emissive states as *ligand-to-ligand* (CT2) as opposed to *ligand-to-silsesquioxane* (CT1) CT states. Our results demonstrate the importance of using RSH functionals and of accounting for solvent effects in modeling the unique spectroscopic properties of this multichromophoric system. Work on elucidating the mechanism and rate of the transition from the absorptive $\pi-\pi^*$ state to the emissive CT2 state is currently underway and will be discussed in a future paper.

■ ASSOCIATED CONTENT

Supporting Information

Energies, γ parameters, optimized geometries, and complete refs 1c and 9. This material is available free of charge via the Internet at http://pubs.acs.org.

■ AUTHOR INFORMATION

Corresponding Author

eitan@umich.edu; bdunietz@umich.edu

Notes

The authors declare no competing financial interest.

■ ACKNOWLEDGMENTS

This work is pursued as part of the Center for Solar and Thermal Energy Conversion, an Energy Frontier Research Center funded by the U.S. Department of Energy Office of Science, Office of Basic Energy Sciences, under 390 Award No. DE-SC0000957. We are grateful for stimulating discussion with Prof. Laine and Prof. Goodson on the optical properties of the functionalized SQs. H.P. acknowledges that this material is supported by the National Science Foundation Graduate Research Fellowship under Grant No. DGE 0718128.

■ REFERENCES

(1) (a) Chan, K. L.; Sonar, P.; Sellinger, A. *J. Mater. Chem.* **2009**, *19*, 9103. (b) Sulaiman, S.; Bhaskar, A.; Zhang, J.; Guda, R.; Goodson, T., III; Laine, R. M. *Chem. Mater.* **2008**, *20*, 5563. (c) Laine, R. M.; et al. *J. Am. Chem. Soc.* **2010**, *132*, 3708. (d) Cho, H.-J.; Hwang, D.-H.; Lee, J.-I.; Jung, Y.-K.; Park, J.-H.; Lee, J.; Lee, S.-K.; Shim, H.-K. *Chem. Mater.* **2006**, *18*, 3780.

(2) (a) Zhen, C.; Becker, U.; Kieffer, J. *J. Phys. Chem. A* **2009**, *113*, 9707. (b) Li, H. C.; Lee, C. Y.; McCabe, C.; Striolo, A.; Neurock, M. *J. Phys. Chem. A* **2007**, *111*, 3577. (c) Lin, T.; He, C.; Yang, X. *J. Phys. Chem. B* **2003**, *107*, 13788.

(3) (a) Reynolds, L.; Gardecki, J. A.; Frankland, S. J. V.; Horng, M. L.; Maroncelli, M. *J. Phys. Chem.* **1996**, *100*, 10337. (b) Ogunsipe, A.; Maree, D.; Nyokong, T. *J. Mol. Struct.* **2003**, *650*, 131.

(4) Hirata, S.; Head-Gordon, M. *Chem. Phys. Lett.* **1999**, *314*, 291.

(5) (a) Livshits, E.; Baer, R. *Phys. Chem. Chem. Phys.* **2007**, *9*, 2932. (b) Baer, R.; Neuhauser, D. *Phys. Rev. Lett.* **2005**, *94*, 043002.

(6) (a) Wu, Q.; Van Voorhis, T. *Phys. Rev. A* **2005**, *72*, 024502. (b) Kaduk, B.; Kowalczyk, T.; Van Voorhis, T. *Chem. Rev.* **2012**, *1*, 321.

(7) (a) Cances, E.; Mennucci, B.; Tomasi, J. *J. Chem. Phys.* **1997**, *107*, 3032. (b) Mennucci, B.; Tomasi, J. *J. Chem. Phys.* **1997**, *106*, 5151.

(8) (a) Lange, A.; Herbert, J. *J. Chem. Phys.* **2010**, *133*, 244111. (b) Lange, A.; Herbert, J. *Chem. Phys. Lett.* **2011**, *509*, 77.

(9) Shao, Y.; et al. *Phys. Chem. Chem. Phys.* **2006**, *8*, 3172.

(10) Stephens, P.; Devlin, F.; Chabalowski, C.; Frisch, M. *J. Phys. Chem.* **1994**, *98*, 11623.

(11) (a) Stein, T.; Kronik, L.; Baer, R. J. *Chem. Phys.* **2009**, *131*, 244119. (b) Kuritz, N.; Stein, T.; Baer, R.; Kronik, L. *J. Chem. Theory Comput.* **2011**, *7*, 2408.

(12) Tozer, D. *J. Chem. Phys.* **2003**, *119*, 12698.

(13) Phillips, H.; Zheng, S.; Hyla, A.; Laine, R.; Goodson, T., III; Geva, E.; Dunietz, B. D. *J. Phys. Chem. A* **2012**, *116*, 1137.

(14) (a) Casida, M. E.; Gutierrez, F.; Guan, J. G.; Gadea, F. X.; Salahub, D. R.; Daudey, J. P. *J. Chem. Phys.* **2000**, *113*, 7062. (b) Hsu, C. P.; Hirata, S.; Head-Gordon, M. *J. Phys. Chem. A* **2001**, *105*, 451.

(15) (a) Bernasconi, L.; Sprik, M.; Hutter, J. *J. Chem. Phys.* **2003**, *119*, 12417. (b) Vaswani, H. M.; Hsu, C. P.; Head-Gordon, M.; Fleming, G. R. *J. Phys. Chem. B* **2003**, *107*, 7940.

(16) Head-Gordon, M.; Grana, A.; Maurice, D.; White, C. *J. Phys. Chem.* **1995**, *99*, 14261.

(17) (a) Perdew, J. P.; Zunger, A. *Phys. Rev. B* **1981**, *23*, 5048. (b) Dreuw, A.; Weisman, J.; Head-Gordon, M. *J. Chem. Phys.* **2003**, *119*, 2943.